

# Order and Dynamics in Lipid Bilayers from 1,2-Dipalmitoyl-*sn*-glycero-phospho-diglycerol as Studied by NMR Spectroscopy

René Lehnert,<sup>†</sup> Hans-Jörg Eibl,<sup>‡</sup> and Klaus Müller<sup>\*,†</sup>

*Institut für Physikalische Chemie, Universität Stuttgart, Pfaffenwaldring 55, D-70569 Stuttgart, Germany, and Max-Planck-Institut für Biophysikalische Chemie, Am Fassberg 11, D-37070 Göttingen, Germany*

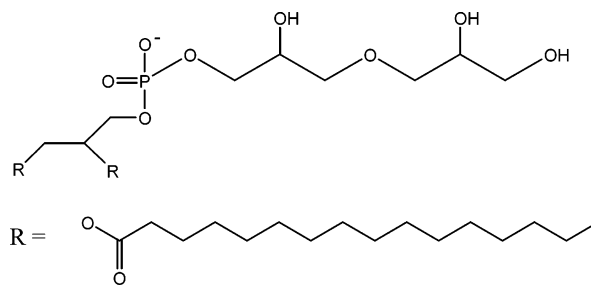
*Received: March 22, 2004; In Final Form: June 6, 2004*

The conformational and dynamic behavior of a new model membrane—1,2-dipalmitoyl-*sn*-glycero-phospho-diglycerol (DPPG<sub>2</sub>)—is studied for the first time by <sup>2</sup>H and <sup>31</sup>P NMR spectroscopy. The investigations are focused on the evaluation of the molecular properties of the lipid molecules as a function of temperature and sample composition. <sup>2</sup>H NMR studies are performed on water dispersions with lipids bearing either selectively deuterated (at position C-6 of both aliphatic chains) or perdeuterated acyl chains. The present studies demonstrate that the introduction of the hydrophilic diglycerol headgroup is accompanied by a reduction of the orientational and conformational order of the acyl chains. The combined analysis of the <sup>2</sup>H NMR line shape and FT IR data—obtained from experiments on DPPG<sub>2</sub> samples with both perdeuterated and selectively deuterated acyl chains—provides the conformational properties of the methylene positions along the fatty acid chains. <sup>2</sup>H NMR line shapes and spin–spin and spin–lattice relaxation data are further analyzed and provide insight into the dynamic features of these model membranes. By means of computer simulations, different motional modes can be distinguished, comprising (overall) anisotropic rotational diffusion, chain isomerization, and lateral diffusion. It is found that the bulky diglycerol headgroup has a significant effect on the molecular mobility of the lipid molecules, as shown by comparison with other lipid systems, such as DMPC and DPPC.

## Introduction

In recent years, solid-state NMR spectroscopy, comprising <sup>2</sup>H, <sup>31</sup>P, <sup>13</sup>C, and <sup>1</sup>H NMR methods, has provided detailed information about the molecular behavior of lipid molecules in model and biological membranes.<sup>1–5</sup> In particular, dynamic NMR techniques have demonstrated their particular suitability for the evaluation of the conformational and ordering features of membrane components, as well as the nature and time scales of the molecular motions in such lipid systems. In this context, especially <sup>2</sup>H NMR spectroscopy on selectively deuterated and perdeuterated compounds has been found to be extremely helpful.<sup>1–3</sup> Thus, the analysis of line shape and relaxation experiments provides access to the various motional contributions in lipid bilayers, which—depending on the actual system—might occur on quite different time scales, ranging from 10<sup>3</sup> to 10<sup>12</sup> s<sup>−1</sup>.

Apart from the dynamic information, <sup>2</sup>H NMR spectroscopy also provides details about the ordering characteristics—in terms of conformational and overall chain order—of the lipid molecules, which normally requires a comprehensive computer-assisted analysis.<sup>1–6</sup> Recently, it has been demonstrated that such ordering quantities are also accessible quite easily from a combined analysis<sup>7–9</sup> of <sup>2</sup>H NMR and FT IR data (e.g., CD<sub>2</sub> rocking band region between 600 and 670 cm<sup>−1</sup><sup>7,10,11</sup>) on lipids with selectively deuterated acyl chains. If on the basis of such an analysis the conformational order throughout the whole acyl chain is known, then in addition the projection length of the alkyl chain on the director can be readily calculated, for which



1,2-dipalmitoyl-*sn*-glycero-3-phosphatidylglycerol (DPPG<sub>2</sub>)

**Figure 1.** Chemical structure of the phospholipid DPPG<sub>2</sub> used in this work.

several theoretical approaches exist.<sup>12–15</sup> Earlier studies have shown that the actual lipid structure, sample composition, and sample temperature (or bilayer phase) have a strong impact on such ordering features.

In this contribution, we present the first comprehensive <sup>2</sup>H and <sup>31</sup>P NMR study on a new synthetic model membrane—1,2-dipalmitoyl-*sn*-glycero-phospho-diglycerol (DPPG<sub>2</sub>, see Figure 1)—which belongs to the group of 1,2-dipalmitoyl-*sn*-glycero-phospho-oligoglycerols (DPPG<sub>x</sub>, *x* = 1, 2, ...).<sup>8</sup> Like the well-known “Stealth” phospholipids,<sup>16–21</sup> the present oligoglycerol phospholipids show a prolonged in vivo blood circulation time and are therefore of considerable interest as drug carriers. The present work addresses the molecular origin of these specific macroscopic properties. For this reason, variable-temperature <sup>2</sup>H NMR line shape and relaxation studies are performed on fully hydrated lipid bilayers with selectively deuterated (at carbon position C-6) or perdeuterated acyl chains. Furthermore, lipid bilayers with a cholesterol content of 40 mol

\* Author for correspondence. Phone: +49(711) 685 4470. FAX: +49-(711) 685 4467. E-mail: k.mueller@ipc.uni-stuttgart.de.

<sup>†</sup> Universität Stuttgart.

<sup>‡</sup> Max-Planck-Institut für Biophysikalische Chemie.

% are examined to reveal the impact of the steroid content on the dynamics and conformational features of the lipid molecules. Additional information about the present systems is obtained by  $^{31}\text{P}$  NMR investigations. The derived molecular parameters for the present DPPG<sub>2</sub> bilayers, obtained via a comprehensive computer-assisted data analysis, are compared with those reported for related lipid systems, such as DMPC (1,2-dimyristoyl-*sn*-glycero-phosphocholine) or DPPC (1,2-dipalmitoyl-*sn*-glycero-phosphocholine).

### Experimental Section

**Materials.** Selectively deuterated and perdeuterated lipids were obtained by the attachment of hexadecanoic acid-6,6-*d*<sub>2</sub> and hexadecanoic acid-*d*<sub>31</sub>, respectively. The selectively deuterated carboxylic acid was prepared in a three-step reaction,<sup>22–24</sup> starting from undecanoic acid. After reduction with  $\text{LiAlD}_4$  (99% deuterated) and bromination, the undecanebromide-1,1-*d*<sub>2</sub> was used in a Grignard reaction with 5-bromovaleric acid to give the desired selectively deuterated hexadecanoic acid (degree of deuteration at position C-6 = 98%). Perdeuterated hexadecanoic acid-*d*<sub>31</sub> was synthesized by repeated, Pt-catalyzed H/D exchange in an autoclave at 200 °C, as described in ref 24. The isotopic enrichment was determined via mass spectrometry, which provided a value of 87% deuteration. In the final step, the deuterated hexadecanoic acid was coupled with the oligoglycerol headgroup to give DPPG<sub>2</sub>. Further details about the preparation of DPPG<sub>2</sub> can be found elsewhere.<sup>24–28</sup>

**Sample Preparation.**<sup>8</sup> Multilamellar, cholesterol-free lipid dispersions were prepared by the addition of 15 mL of deuterium-depleted water to 10 mg of lipid to ensure complete hydration of the diglycerol headgroup. Homogenization was obtained by repeated freeze–thawing, centrifuging, vortexing, and incubation for about 3 h at temperatures well above the main transition of the membrane. The cholesterol-containing dispersions were prepared by dissolving the appropriate amounts of lipid and cholesterol (40% molar ratio) in a small quantity of freshly distilled chloroform. The solvent was removed in a dry nitrogen stream, followed by evaporation in a vacuum for a few hours. The subsequent hydration and freeze–thawing steps were carried out as described above.

**NMR Measurements.**  $^2\text{H}$  NMR and  $^{31}\text{P}$  NMR measurements were carried out on a CXP 300 NMR spectrometer (Bruker, Karlsruhe, Germany) at resonance frequencies of 46.01 and 121.5 MHz, respectively, using a commercial double resonance probe. The spectrometer was controlled by a MacSpect unit (Tecmag, Houston, TX) and was equipped with a 1 kW linear amplifier (LPI-10H, ENI, Rochester, NY). The  $B_1$  field strengths were adjusted to give  $\pi/2$  pulse lengths of 2 and 3  $\mu\text{s}$  for  $^2\text{H}$  and  $^{31}\text{P}$ , respectively.

$^2\text{H}$  NMR spectra and spin–spin relaxation times ( $T_2$ ) were obtained employing the quadrupole echo sequence,  $(\pi/2)_x - \tau_e - (\pi/2)_y - \tau_e - \text{acq}$ . The  $^2\text{H}$  NMR line shapes were recorded at a fixed delay between the  $\pi/2$  pulses of 20  $\mu\text{s}$ . The recycle delay varied between 0.3 s in the liquid crystalline phase and 8 s in the gel phase. Spin–lattice relaxation times ( $T_1$ ) were obtained by a modified inversion–recovery sequence,  $(\pi) - \tau_r - (\pi/2)_x - \Delta - (\pi/2)_y - \Delta - \text{acq}$ . Here, the initial  $\pi$  pulse was replaced by a composite pulse, as described elsewhere.<sup>29</sup>

All  $^{31}\text{P}$  NMR experiments were performed in the presence of broadband proton decoupling (decoupling power = 20 and 55 W in the liquid crystalline phase and gel phase, respectively).  $^{31}\text{P}$  spin–spin relaxation times were measured using the spin–echo sequence  $(\pi/2) - \tau_e - (\pi) - \tau_e - \text{acq}$ , and the spin–lattice relaxation times were determined via a saturation–recovery sequence. The recycle delay was between 6 s (liquid crystalline

phase) and 100 s (gel phase). The sample temperature during the variable-temperature experiments was controlled with a Bruker BVT 1000 temperature control unit. To obtain the exact sample temperature, an external temperature calibration was performed prior to the NMR measurements by placing a thermocouple in the NMR sample coil. The temperature stability was found to be within  $\pm 1$  K.

**Data Processing and Simulations.** FORTRAN programs have been developed that describe the behavior of isolated  $I = 1$  spin systems during the corresponding pulsed NMR experiments.<sup>9,30–32</sup> Theoretical  $^2\text{H}$  NMR line shapes, spin–spin and spin–lattice relaxation rates were obtained by a numerical diagonalization of the corresponding relaxation matrices. The  $^2\text{H}$  NMR line shape and spin–spin relaxation simulations in the gel phase are based on the model of the anisotropic rotational diffusion.<sup>33</sup> Here, a rotational diffusion process<sup>34–37</sup> was assumed that is described by a rotation about the long molecular axis in the presence of a restricted fluctuation of the long molecular axis in an ordering potential,<sup>33</sup> with the main axis given by the liquid crystalline director axis. It should be noted that the rotational motion was further simplified by the assumption of a degenerate three-site jump process. For the molecular fluctuations next-neighbor jumps were assumed. The ordering potential is directly related to the orientational order parameter  $S_\alpha$  that gives rise to unequally populated fluctuation sites.<sup>34–37</sup> The ordering potential is given by

$$V_{\text{pot},i} = A_{\text{ord}} \cos \left[ (i - 0.5) \frac{\pi}{2N} \right]^2 \quad i = 1, \dots, N \quad (1)$$

Here,  $N$  refers to the number of possible orientations, which in the present work was fixed to 30. The potential depth  $A_{\text{ord}}$  is connected to the orientational order parameter  $S_\alpha$  by<sup>38</sup>

$$S_\alpha = \frac{\int_0^\pi \frac{1}{2} (3 \cos^2 \Theta - 1) \exp(A_{\text{ord}} \cos^2 \Theta) \sin \Theta \, d\Theta}{\int_0^\pi \exp(A_{\text{ord}} \cos^2 \Theta) \sin \Theta \, d\Theta} \quad (2)$$

The given number of fluctuation sites  $N$  emerged from a series of model simulations using different order parameters  $S_\alpha$  and numbers of sites. The value of  $N = 30$  ensures that the  $^2\text{H}$  NMR line shapes converge and thus do not depend on the number of fluctuation sites.

The  $^2\text{H}$  NMR spin–spin relaxation data in the liquid crystalline phase were analyzed with the assumption of a lateral lipid motion within the bilayers across the curved surface. For the simulation of these data, an isotropic rotational diffusion model was employed, as reported for other lipid systems.<sup>39–41</sup>

The  $^2\text{H}$  spin–lattice relaxation data in the gel phase below 300 K were reproduced by employing two motional contributions. From the overall reorientational motions only the aforementioned overall rotation (degenerate three-site jump process) was considered, whereas molecular fluctuations—due to the high orientational order parameter—were neglected. The second contribution is a mutual two-site jump process between gauche<sup>−</sup> and gauche<sup>+</sup> sites at position C-2 of the *sn*-2 chain that affects all other acyl chain segments in the same way and that are populated to 60 and 40%, respectively, as described previously.<sup>35,42</sup>

### Results

In the following, we report the results of a comprehensive  $^2\text{H}$  NMR and  $^{31}\text{P}$  NMR study on bilayers from 1,2-dipalmitoyl-*sn*-glycero-phospho-diglycerol (DPPG<sub>2</sub>). DSC measurements

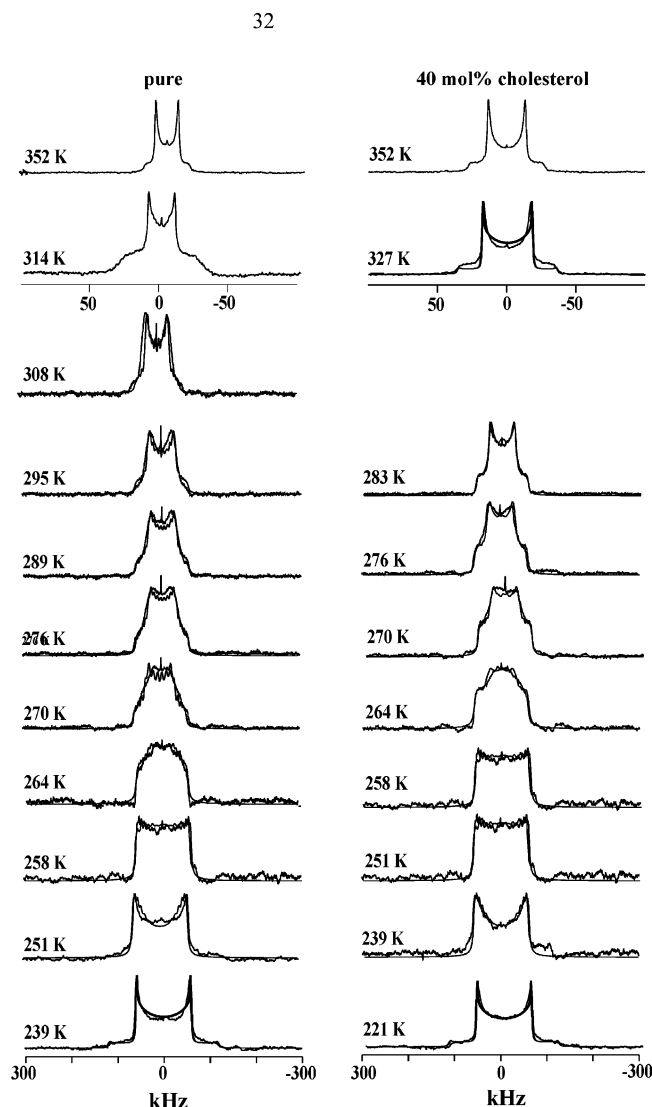


**Figure 2.** Variable-temperature  $^2\text{H}$  NMR line shapes of DPPG<sub>2</sub>-6,6- $d_2$  above and below the main phase transition. Left column, pure lipid/water dispersion; right column, mixture with 40 mol % cholesterol. In addition, the simulated spectra are superimposed (see text).

were carried out to understand the phase behavior of the present DPPG<sub>2</sub> samples. It was found that the main transition temperature of pure DPPG<sub>2</sub>/water dispersions occurs at  $T_m = 314$  K, as also reported for the reference system DPPG<sub>1</sub> (= DPPG). The incorporation of 40 mol % cholesterol leads to a broadening of the phase transition between 300 and 320 K (error of phase transition temperature =  $\pm 0.5$  °C).<sup>8</sup>

**$^2\text{H}$  NMR Line Shapes and Order Parameters.** In Figure 2, representative  $^2\text{H}$  NMR spectra are given for multilamellar dispersions of DPPG<sub>2</sub> (left column) and DPPG<sub>2</sub>/cholesterol (right column), deuterated at position C-6 of both fatty acid chains. In addition, the experimental  $^2\text{H}$  NMR line shapes of the gel phase are superimposed by the theoretical spectra from the computer simulations, using the motional models and parameters as mentioned in the Experimental Section and the text below. As for other lipids, in the liquid crystalline state, the  $^2\text{H}$  NMR spectra of the present systems are characterized by rather narrow, axially symmetric powder line shapes that reflect a high mobility of the lipid molecules. For the cholesterol-free bilayers, a quadrupolar splitting of 18 kHz is observed at 333 K, whereas the sample with cholesterol shows a splitting of 32 kHz at this temperature. This is due to the known ordering effect of the steroid on the hydrophobic part of the bilayer.

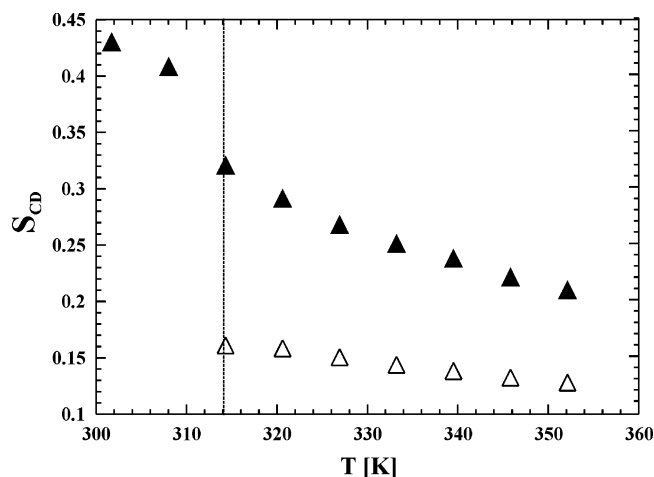


**Figure 3.** Derived order parameter  $S_{\text{CD}}$  for DPPG<sub>2</sub>-6,6- $d_2$  bilayers in the pure sample ( $\Delta$ ) and in the mixture with 40 mol % cholesterol ( $\blacktriangle$ ). The phase transition temperature is marked by a dotted line at 314 K.

Unlike other phospholipid/water dispersions, no pronounced inequivalence of the *sn*-1 and *sn*-2 chains is found, as just one quadrupolar splitting can be resolved. Upon lowering the sample temperature, an increase of the quadrupolar splitting in both samples is registered. At the phase transition temperature  $T_m$ , the  $^2\text{H}$  NMR spectra of the pure lipid/water dispersions change dramatically. Here, a narrow “high-temperature” component and a second “low-temperature” component with a quadrupolar splitting of 45 kHz is observed, which is caused by a discontinuous slowing of the underlying motional processes. The high-temperature component disappears completely at around 5 K below the main phase transition, i.e., here, only the broad low-temperature component remains. The  $^2\text{H}$  NMR line shapes are subject to significant changes between 289 and 251 K, until at 239 K an almost static  $^2\text{H}$  NMR spectrum with a quadrupolar splitting of about 120 kHz is registered, which is typical for lipid molecules being rigid on the NMR time scale. In the case of the sample with 40 mol % cholesterol, no such discontinuity is observed around  $T_m$ . Rather, the  $^2\text{H}$  NMR line shapes become steadily broader until about 276 K. Below this temperature the sample with cholesterol undergoes the same spectral changes as found for the pure DPPG<sub>2</sub>/water dispersion. Eventually, at 221 K, a rigid powder pattern with a quadrupolar splitting of 120 kHz is again registered.

In the liquid crystalline phase (“fast motional limit”), the overall order parameter  $S_{\text{CD}}$  is directly derived from the experimental  $^2\text{H}$  NMR spectra. In this temperature range,  $S_{\text{CD}}$  is related to the experimental quadrupolar splitting  $\Delta\nu_q$  between the perpendicular singularities by<sup>1</sup>

$$\Delta\nu_q = -\frac{3}{4}\left(\frac{e^2qQ}{h}\right)S_{\text{CD}} \quad (3)$$

where  $e^2qQ/h$  is the static quadrupolar coupling constant with a typical value of 167 kHz for an aliphatic C–D bond. Figure 3 summarizes the temperature-dependent order parameter  $S_{\text{CD}}$  as the absolute value for both DPPG<sub>2</sub> samples, as derived from the experimental  $^2\text{H}$  NMR line shapes. In general,  $S_{\text{CD}}$  is found to increase with decreasing temperature. Hence, for the pure system, values of 0.13 (352 K) and 0.16 (314 K) are observed. The incorporation of 40 mol % cholesterol significantly increases the order parameter  $S_{\text{CD}}$ , as reflected by values between 0.21 (352 K) and 0.32 (314 K). Because of the existence of a “liquid-ordered” phase<sup>43</sup> in the sample with cholesterol,  $S_{\text{CD}}$  can be determined even at temperatures below  $T_m$  of the pure bi-

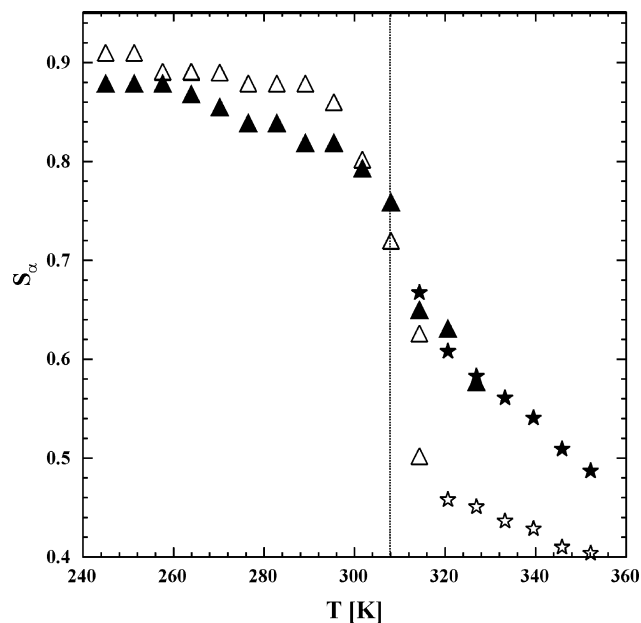


**Figure 4.** Orientational order parameter  $S_\alpha$  in DPPG<sub>2</sub>-6,6- $d_2$  as derived from  $^2\text{H}$  NMR  $T_2$  and line shape simulation ( $\Delta$ ,  $\blacktriangle$ ), and a combined  $^2\text{H}$  NMR and FTIR data analysis ( $\star$ ,  $\star$ ). Open and filled symbols refer to the pure bilayer system and the mixture with 40 mol % cholesterol, respectively. The main phase transition temperature of the pure lipid bilayer is marked by a dotted line.

layer sample. The lowest accessible temperature with a “fast exchange”  $^2\text{H}$  NMR line shape is 300 K, at which  $S_{\text{CD}}$  is given as 0.43.

A second quantity that characterizes the liquid crystalline order is the orientational order parameter  $S_\alpha$ . Figure 4 exhibits the derived values for the present DPPG<sub>2</sub> samples including the data both below and above the main phase transition. The data below the main transition were obtained via  $^2\text{H}$  NMR line shape analysis, based on the model assumptions outlined in the Experimental Section and in the next section. The data above the main phase transition were deduced from the combined analysis of the FT IR and  $^2\text{H}$  NMR data for the same sample, deuterated at carbon position C-6, using eqs 4 and 5.<sup>7,12</sup>

$$S_{\text{CD}} = S_\alpha S_\gamma \quad (4)$$

$$S_\gamma = -\frac{1}{2}p_t \quad \text{with } p_t = 1 - p_g \quad (5)$$

Here,  $p_t$  and  $p_g$  are the trans and gauche populations, respectively. The gauche populations  $p_g$  were directly derived from the analysis of the  $\text{CD}_2$  rocking modes, as described previously by Mendelsohn et al.<sup>11</sup> For the present DPPG<sub>2</sub> samples, these data are reported in a former comprehensive variable-temperature FT IR study.<sup>8</sup>

In the gel phase,  $S_\alpha$  values of about 0.9 (242 K) for the pure lipid/water dispersions and slightly lower values of about 0.89 (242 K) for the mixture with cholesterol are obtained. At the phase transition, the order parameter of the pure lipid membrane drops considerably to a value of 0.5 at 314 K. A further temperature increase results in a continuous reduction of  $S_\alpha$ , with a value of 0.4 at the upper temperature limit at 352 K. For the mixture with cholesterol, the drop at the main phase transition is less pronounced. Here, above  $T_m$ , orientational order parameters  $S_\alpha$  between 0.45 and 0.67 are observed, reflecting a similar continuous reduction with increasing sample temperature.

In addition, DPPG<sub>2</sub> samples with perdeuterated acyl chains were examined, from which (see eq 3) the order parameter  $S_{\text{CD}}$

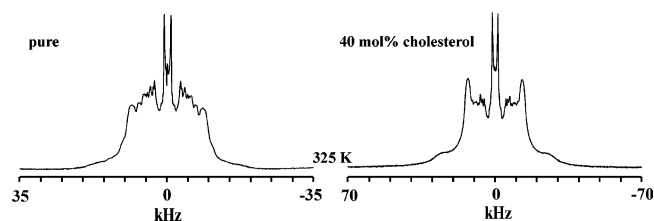


**Figure 5.** Representative  $^2\text{H}$  NMR line shapes of DPPG<sub>2</sub> with perdeuterated acyl chains above the main phase transition at 325 K.

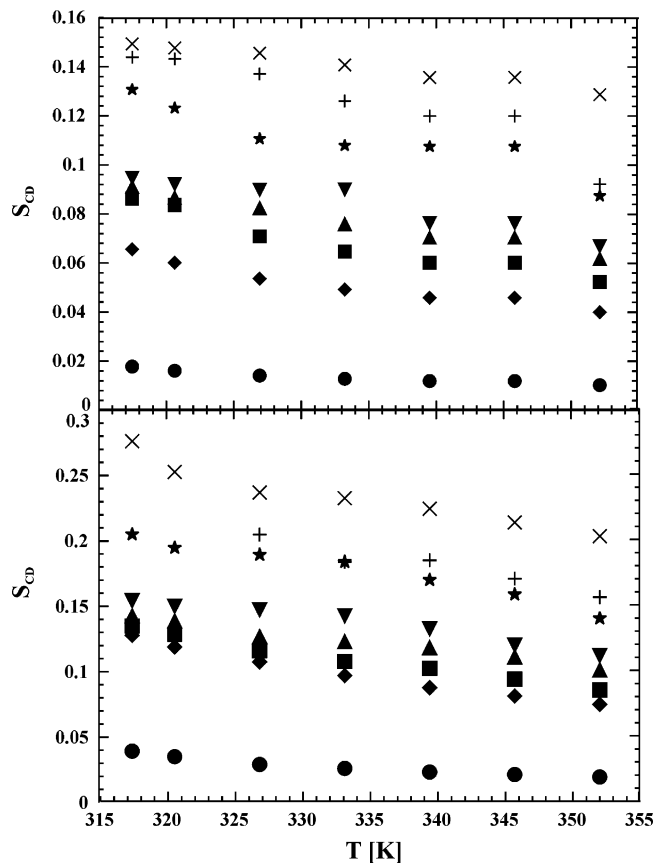


**Figure 6.** Order parameter  $S_{\text{CD}}$  for DPPG<sub>2</sub> derived from the samples with perdeuterated acyl chains: (x) plateau region C2–C9, (+) C10, (\*) C11, (v) C12, (A) C13, (■) C14, (♦) C15, (●) C16. Top graph, pure lipid/water bilayer; lower graph, mixture with 40 mol % cholesterol.

for the methylene segments along the fatty acid chains could be derived. Figure 5 shows representative  $^2\text{H}$  NMR line shapes for the pure and the cholesterol-rich samples at  $T = 323$  K. Figure 6 summarizes the derived  $S_{\text{CD}}$  values for the various assigned positions and the plateau region, covering carbon positions C-2 to C-9. In agreement with previous reports,<sup>15,44</sup>  $S_{\text{CD}}$  decreases with temperature and along the fatty acid chain from the plateau region toward the chain end (carbon position C-16). For the plateau region of the pure DPPG<sub>2</sub> bilayers, values between 0.13 (352 K) and 0.15 (317 K) are obtained. These values are consistent with the aforementioned values for the C-6 position in the selectively deuterated sample. For the chain end (position C-16), significantly lower values were derived (0.03 at 352 K, 0.06 at 317 K). The values for the mixture with cholesterol are found to be about 80% higher, which can be attributed to the ordering effect of the steroid.

With the orientational order parameter  $S_\alpha$  from above (Figure 4) and the position-dependent  $S_{\text{CD}}$  order parameters (Figure 6), it is possible to calculate the position-dependent segmental order



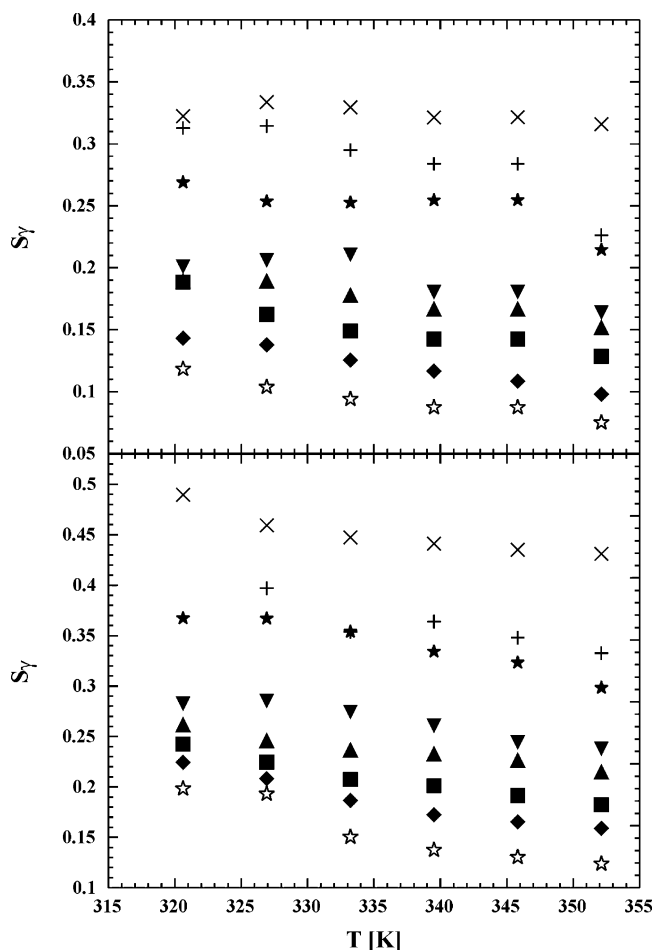


**Figure 7.** Segmental order parameter  $S_\gamma$  as derived from the combined  $^2\text{H}$  NMR and FTIR analysis for the various positions along the acyl chains: (x) plateau region C2–C9, (+) C10, (\*) C11, (▼) C12, (▲) C13, (■) C14, (◆) C15, (☆) C16. Top graph, pure lipid/water bilayer; lower graph, mixture with 40 mol % cholesterol.

parameter  $S_\gamma$  for the whole acyl chain using eq 4. Figure 7 summarizes the derived  $S_\gamma$  values for both the pure DPPG<sub>2</sub>/water dispersion and the mixture with cholesterol in the liquid crystalline phase. For the pure lipid/water dispersion, values between 0.33 (326 K) for the plateau region, i.e., carbon positions C-2 to C-9, and 0.09 (326 K) at C-16 are observed that again decrease with increasing sample temperature. The addition of 40 mol % cholesterol increases the segmental order parameters  $S_\gamma$  considerably, as reflected by the value of 0.45 for the plateau region at 326 K.

As the order parameter  $S_\gamma$  can be related via eq 5 to the probability that the segment is in a gauche conformational state, it is possible to calculate an effective chain length as a projection on the liquid crystal director axis, following the model assumptions described in the Appendix. In fact, we have calculated the effective acyl chain length in DPPG<sub>2</sub> using three different approaches: (i) the model of Petersen and Chan<sup>12</sup> for the determination of  $S_\gamma$  along with the method of Oldfield<sup>44</sup> for the calculation of the effective chain length, (ii) the diamond-lattice model suggested by Seelig et al.,<sup>13,14,45</sup> and (iii) the first-order mean-torque model of Petrache et al.<sup>15,46</sup>

Table 1 and Figure 8 summarize the results for the pure DPPG<sub>2</sub>/water dispersion and the mixture with cholesterol. The Petersen/Chan approach provides chain lengths between 12.0 Å at 321 K and 11.1 Å at 352 K for the pure lipid bilayer. The incorporation of 40 mol % cholesterol increases the projection

**TABLE 1: Effective Acyl Chain Lengths Derived for DPPG<sub>2</sub> Bilayers**

$T$ (K)	method I: Chan/Oldfield <sup>a</sup>	method II: Seelig <sup>b</sup>	method III: Petrache <sup>c</sup>
Pure Lipid/Water Bilayers			
352	11.1	11.2	9.5
346	11.4	11.3	10.0
340	11.5	11.3	10.1
333	11.7	11.4	10.4
327	11.8	11.5	10.6
321	12.0	11.6	10.9
Mixture with 40 mol % Cholesterol			
352	13.0	12.3	11.9
346	13.2	12.4	12.2
340	13.3	12.6	12.5
333	13.5	12.7	12.7
327	13.8	12.9	13.2
321	14.0	12.8	13.6

<sup>a</sup> Petersen, N. O.; Chan, S. I. *Biochemistry* **1977**, *16*, 2657. Oldfield, E.; Meadows, M.; Rice, D.; Jacobs, R. *Biochemistry*, **1978**, *17*, 2727.

<sup>b</sup> Seelig, A.; Seelig, J. *Biochemistry* **1974**, *13*, 4839. Schindler, H.; Seelig, J. *Biochemistry* **1975**, *14*, 2283. Seelig, J.; Seelig, A. *Quart. Rev. Biophys.* **1980**, *13*, 337. <sup>c</sup> Petrache, H. I.; Tu, K.; Nagle, J. F. *Biophys. J.* **1999**, *76*, 2479. Petrache, H. I.; Dodd, S. W.; Brown, M. F. *Biophys. J.* **2000**, *79*, 3172.

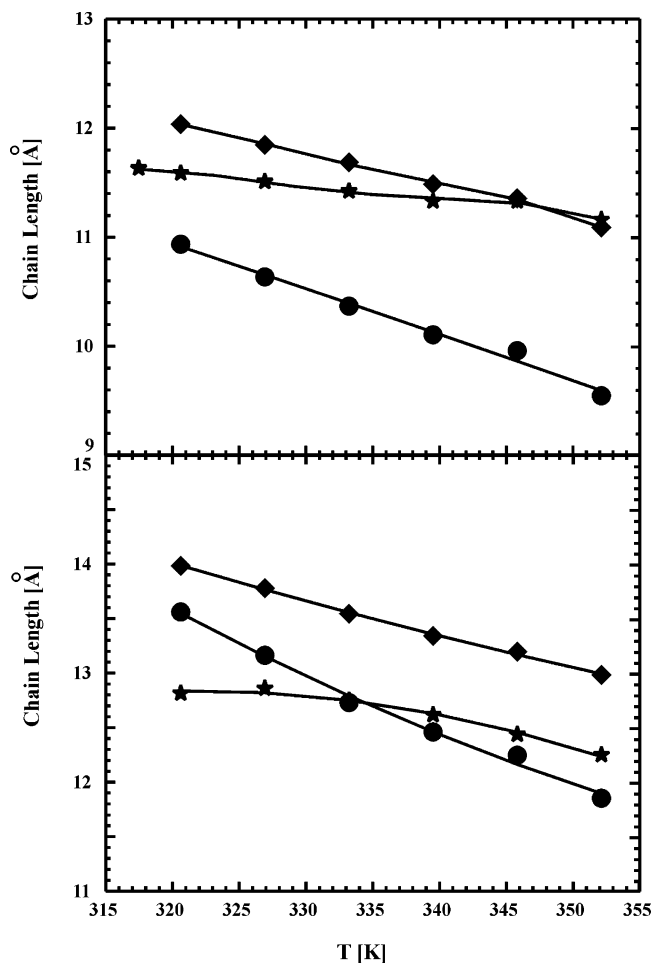


**Figure 8.** Calculated effective acyl chain lengths versus temperature using different approaches (see text). (◆) model I (Chan, Oldfield), (\*) model II (Seelig), (●) model III (Petrache, Brown). Top graph, pure lipid/water bilayer; lower graph, mixture with 40 mol % cholesterol.

length by about 10%. Similar values are found on the basis of the model proposed by Seelig et al.<sup>13,14,45</sup> Here, at 321 K, an effective chain length of 11.4 Å for the pure bilayer is obtained.

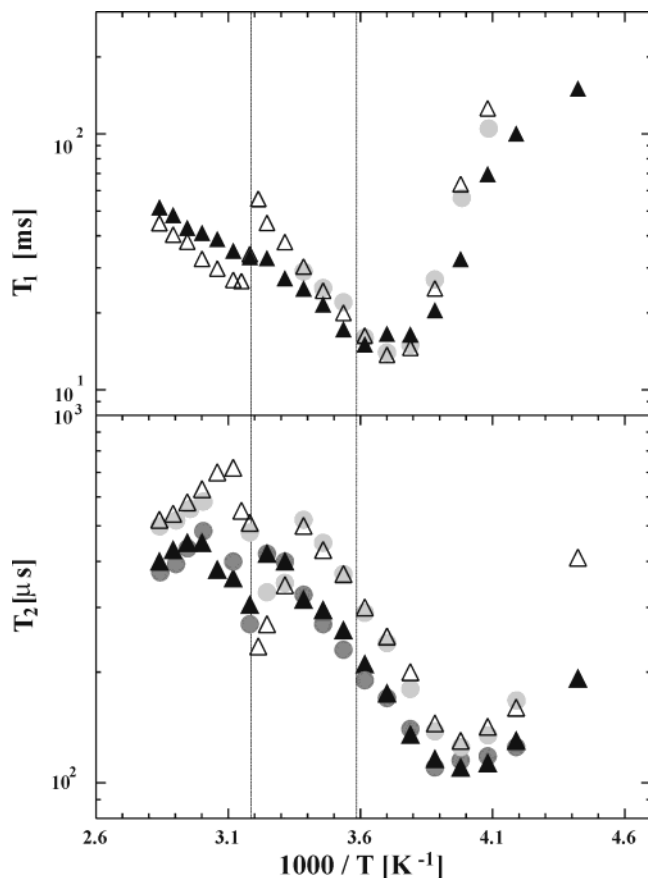


**Figure 9.** Experimental  $^2\text{H}$   $T_1$  (top graph) and  $T_2$  (lower graph) data of DPPG<sub>2</sub>-6,6- $d_2$ : pure lipid/water dispersion ( $\Delta$ ), mixture with 40 mol % cholesterol ( $\blacktriangle$ ). The main phase transition of the pure lipid bilayer (314 K) and the freezing temperature of water are marked with dotted lines. The corresponding theoretical results are also given by gray circles.

The chain length decreases upon heating to 352 K to reach a limiting value of 10.7 Å. Again, the incorporation of 40 mol % cholesterol increases the chain length by about 12%. It is obvious that the first-order mean-torque model provides the lowest values over the whole temperature range. This holds in particular for higher sample temperatures with a low order parameter  $S_{\text{CD}}$ , where the projection lengths lie between 10.9 Å (321 K) and 9.5 Å (352 K). In this case, addition of 40 mol % cholesterol increases the effective chain length by 20% as compared to the pure DPPG<sub>2</sub>/water bilayer.

**Line Shape Analysis and Lipid Dynamics.**  $^2\text{H}$  spin–spin and spin–lattice relaxation times were measured for the pure lipid/water dispersion and the mixture with cholesterol, containing DPPG<sub>2</sub> with selectively deuterated acyl chains (carbon position C-6). The  $^2\text{H}$  spin–spin relaxation times, given in Figure 9, exhibit a slight decrease upon heating within the liquid crystalline phase. For the pure lipid/water dispersion the values range from 520  $\mu\text{s}$  (352 K) to 720  $\mu\text{s}$  (320 K). The cholesterol-rich model membrane shows the same temperature dependence but somewhat lower values, i.e., 400  $\mu\text{s}$  at 352 K and 450  $\mu\text{s}$  at 333 K. Upon entering the gel phase at around 314 K, the values of both systems drop to a local minimum with values of 270  $\mu\text{s}$  (308 K) for the pure system and 305  $\mu\text{s}$  (314 K) for the mixture with cholesterol. Further cooling of the samples causes a slight increase of the  $T_2$  data in both systems. At 295 K, the spin–spin relaxation times of both systems again decrease with decreasing temperature, reaching a  $T_2$  minimum at 251 K with values of 130 and 110  $\mu\text{s}$  for the pure lipid bilayer and the

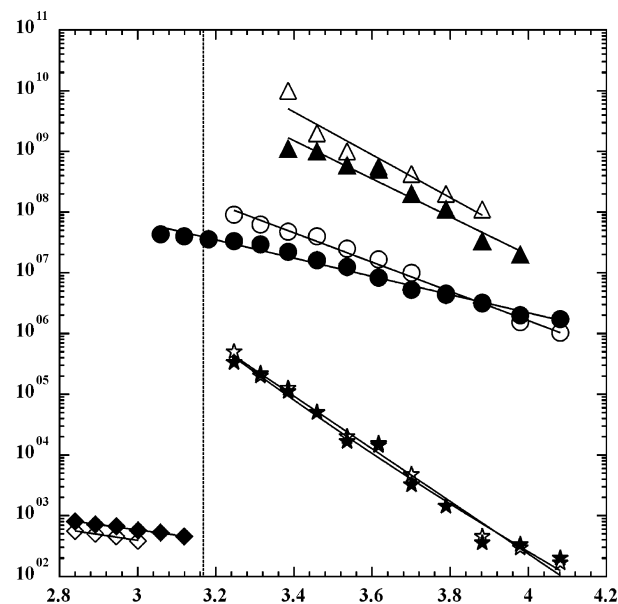


**Figure 10.** Arrhenius plots of the correlation times for the derived motions in DPPG<sub>2</sub>-6,6- $d_2$ : lateral diffusion ( $\diamond, \blacklozenge$ ), chain fluctuation ( $\star, \blackstar$ ) chain rotation ( $\circ, \bullet$ ),  $\text{gauche}^+$ – $\text{gauche}^-$  isomerization at chain segment C-2 ( $\triangle, \blacktriangle$ ). Open and filled symbols refer to the data for the pure lipid/water dispersion and the mixture with 40 mol % cholesterol, respectively. The main phase transition temperature of the pure lipid bilayers is marked by a dotted line.

mixture with cholesterol, respectively. As the  $^2\text{H}$  NMR line shapes and  $T_2$  relaxation times are sensitive to the same motional region, a consistent theoretical reproduction of these experimental data thus requires the use of the same simulation parameters. In fact, for the present bilayer systems, such a consistent data analysis was feasible. Thus, the  $^2\text{H}$  NMR line shapes and spin–spin relaxation data in the gel phase were simulated using the model of anisotropic rotational diffusion,<sup>6,34–37</sup> in close agreement with former studies on DMPC bilayers.<sup>6,34,35</sup> Likewise, for the liquid crystalline phase a reproduction of the  $^2\text{H}$  spin–spin relaxation data was achieved with the assumption that lateral diffusion of the lipid molecule along the curved surface of the vesicles<sup>39–41</sup> provides the dominant relaxation contribution. The theoretical  $^2\text{H}$  NMR spectra based on these assumptions are also given in Figure 2, and in Figure 9, the theoretical  $T_2$  data are compared with their experimental counterparts. The derived correlation times are summarized in the Arrhenius representation in Figure 10.

As shown by the data in Figure 9, in the liquid crystalline phase, both DPPG<sub>2</sub> bilayer systems exhibit a decrease of the  $^2\text{H}$   $T_1$  relaxation data with decreasing sample temperature. Here, the values for the pure lipid/water dispersion decrease from 45 ms at 352 K to a value of 27 ms at 320 K, and at the transition to the gel phase, a discontinuity of the  $T_1$  data can be found. Within the gel phase, the  $^2\text{H}$   $T_1$  data for the pure lipid/water dispersion exhibit a pronounced minimum at 270 K with a  $T_1$  value of 14 ms. The incorporation of 40 mol % cholesterol mainly affects the  $^2\text{H}$   $T_1$  data at higher temperatures, i.e., in the liquid crystalline phase and at the transition to the gel phase, whereas at lower temperatures, the  $T_1$  data remain almost unaltered. Thus, the  $T_1$  minimum with a value of 15 ms practically coincides with the aforementioned minimum found for the pure lipid/water dispersion. Figure 9 also contains the theoretical  $T_1$  relaxation times for both systems, which were obtained with the known rate constants for overall chain rotation (from  $^2\text{H}$  NMR line shape,  $T_2$  simulations) and with the assumption of a two-site jump process between  $\text{gauche}^+$  and

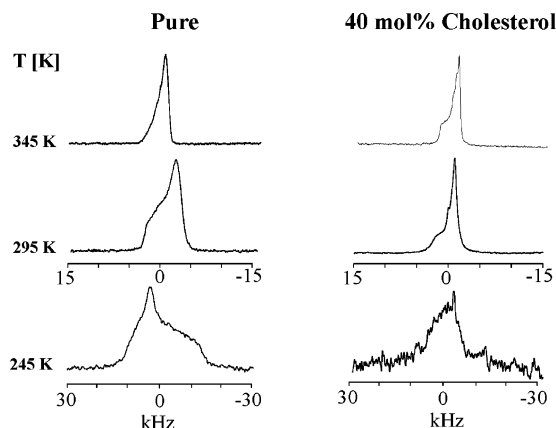
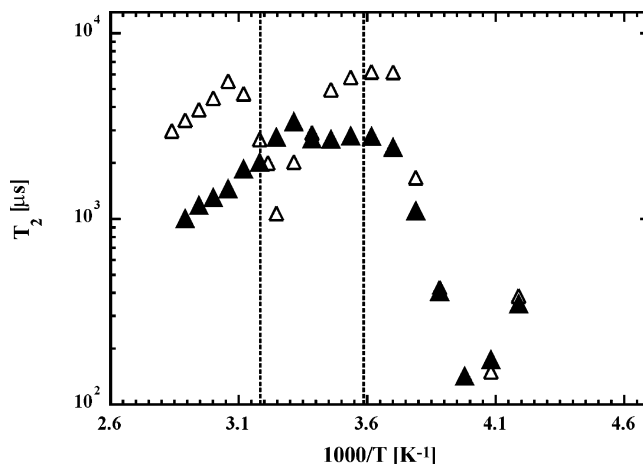
**TABLE 2: Activation Energies for Lipid Motions in DPPG<sub>2</sub> Bilayers**

	$T \leq 300$ K			$T \geq 314$ K
	overall rotation (kJ/mol)	overall fluctuation (kJ/mol)	gauche <sup>+</sup> –gauche <sup>−</sup> isomerization at position C-2 (kJ/mol)	lateral diffusion (kJ/mol)
pure lipid/water dispersion	46.1 ± 1.5	82.9 ± 2.7	67.5 ± 8.0	16.6 ± 0.7
mixture with 40 mol % cholesterol	28.8 ± 1.1	80.5 ± 3.8	60.0 ± 4.7	18.6 ± 1.6

gauche<sup>−</sup> conformers at the C-2–C-3 bond. The latter motional contribution is known to be a major source for <sup>2</sup>H spin–lattice relaxation in such lipid systems.<sup>35,42</sup>

In Figure 10, the derived correlation times for the various motional contributions are plotted in an Arrhenius representation, and the corresponding activation energies are listed in Table 2. In the gel phase, the two-site exchange process between gauche<sup>+</sup> and gauche<sup>−</sup> states exhibits rate constants between  $1 \times 10^{10}$  and  $5 \times 10^8$  s<sup>−1</sup> with activation energies of 67.5 kJ/mol for the pure lipid bilayers and 60.0 kJ/mol for the mixture with cholesterol. Likewise, for the overall lipid rotation in both DPPG<sub>2</sub> samples, similar rate constants between about  $10^6$  and  $10^8$  s<sup>−1</sup> are observed along with activation energies of 46.1 kJ/mol (pure lipid bilayer) and 28.8 kJ/mol (mixture with cholesterol). For the chain fluctuation, almost identical rate constants for the two systems are derived. Here, the activation energies are 82.9 kJ/mol for the pure lipid/water dispersion and 80.5 kJ/mol for the mixture with cholesterol. As mentioned earlier, in the liquid crystalline phase, the spin–spin relaxation could be reproduced using the model of the lateral diffusion of the lipid molecules along the curved surface of the lipid bilayer. Here, rate constants between  $3 \times 10^2$  s<sup>−1</sup> (321 K) and  $9 \times 10^2$  s<sup>−1</sup> (352 K) are obtained for the sample with cholesterol that in general exhibits some smaller values. The activation energies are determined to be 16.6 and 18.6 kJ/mol for the pure DPPG<sub>2</sub>/water dispersion and for the mixture with cholesterol, respectively.

Apart from the <sup>2</sup>H NMR studies described above, <sup>31</sup>P NMR line shape and spin–echo experiments were carried out (see Figures 11 and 12). In Figure 11, representative <sup>31</sup>P NMR line shapes are given. Unfortunately, it turned out that the orientation of the chemical shift tensor relative to the molecular long axis is different from that reported in the literature,<sup>47</sup> which—because of the lack of samples with oriented bilayers—made a quantitative analysis of the <sup>31</sup>P NMR line shapes and relaxation data impossible. Above the main phase transition, both systems exhibit axially symmetric line shapes with a chemical shift anisotropy of about 3.9 kHz for the pure system and about 4.5 kHz for the mixture with cholesterol. In the liquid crystalline phase, the <sup>31</sup>P spin–spin relaxation data (Figure 12) show a constant increase with decreasing temperature, with values of about 3000 μs for the pure lipid/water dispersion and 1000 μs for the mixture with cholesterol. For the pure lipid bilayer below the main phase transition, a sudden increase of the chemical shift anisotropy is visible along with a drop of the <sup>31</sup>P spin–spin relaxation times, in quite the same way as found earlier for the <sup>2</sup>H spin–spin relaxation data. In marked contrast, the mixture with cholesterol exhibits a more continuous change of the <sup>31</sup>P NMR line shapes and <sup>31</sup>P spin–spin relaxation data in the vicinity of the main phase transition. At around 273 K, the <sup>31</sup>P spin–spin relaxation times in both systems experience a sudden drop resulting in a common minimum at around 252 K with a value of 200 μs.

**Figure 11.** Variable-temperature <sup>31</sup>P NMR line shapes of DPPG<sub>2</sub> above and below the main phase transition. Left column, pure lipid/water dispersion; right column, mixture with 40 mol % cholesterol.**Figure 12.** <sup>31</sup>P  $T_2$  data of DPPG<sub>2</sub> in the pure lipid/water dispersion (Δ) and in the mixture with 40 mol % cholesterol (▲). The main phase transition of the pure lipid bilayers (314 K) and the freezing temperature of water are marked with dotted lines.

## Discussion

**Phospholipid Dynamics.** Previous investigations on bilayer membranes have demonstrated that several local and overall motions are necessary to provide a satisfactory description of the corresponding NMR line shape and relaxation data in such systems.<sup>1–5,35,48</sup> Hence, the following types of motion are frequently discussed in phospholipid membranes: (i) trans–gauche isomerization of the methylene segments in the acyl chains, (ii) conformational motions of the glycerol backbone, (iii) rotations around bonds linking the phosphate headgroup with the glycerol backbone, (iv) overall reorientations (rotation and fluctuations) of the lipid molecules, (v) collective order fluctuations, and (vi) lateral diffusion of the lipid molecules within the layers. Of course, the whole variety of motional contributions is accessible only by a comprehensive analysis of the experimental data acquired by different NMR probe nuclei that examine different regions of the lipid molecules. In the present case, the information on the DPPG<sub>2</sub> dynamics is mainly based on the analysis of variable-temperature <sup>2</sup>H NMR experiments, obtained for samples with DPPG<sub>2</sub> bearing selectively deuterated acyl chains. <sup>31</sup>P NMR line shape and spin–spin relaxation studies have been carried out as well, which, however, are discussed only on a qualitative level.

(a) *Liquid Crystalline Phase.* Both the pure DPPG<sub>2</sub>/water dispersion and the mixture with 40 mol % cholesterol exhibit a decrease of the respective <sup>2</sup>H and <sup>31</sup>P  $T_2$  relaxation data with

increasing sample temperature. At the same time, motionally narrowed, axially symmetric  $^2\text{H}$  NMR line shapes are observed, which clearly implies that some lipid motions occur in the fast exchange limit. As shown during earlier studies on DMPC bilayers, the fast motional contributions can be ascribed to overall chain reorientations as well as trans–gauche isomerization.<sup>6,34–36</sup> Furthermore, the lowering of the  $T_2$  values with increasing sample temperature can be traced back to lateral diffusion of the lipid molecules across the curved surface of the bilayer.<sup>39–41</sup> The rate constants for this latter process, obtained from the analysis of the  $^2\text{H}$  line shape and  $T_2$  data (see Figure 10), are found to be on the same order as the published data for other lipid bilayers.<sup>6,49–52</sup> However, the activation energies of about 17 kJ/mol (pure bilayers) and 19 kJ/mol (mixture with cholesterol) are approximately 10 kJ/mol lower than typical values for such bilayer systems. At best, these findings can be related to the low conformational order of the DPPG<sub>2</sub> bilayers (see below), along with a reduced packing density of the acyl chains. This implies that the lateral mobility of the lipid molecules is thermally less hindered, in full agreement with the experimental observations.

(b) *Gel Phase.* In the gel phase, the experimental  $^2\text{H}$  NMR data (line shape, spin–spin relaxation times) for both the pure DPPG<sub>2</sub>/water dispersion and the corresponding mixture with cholesterol are found to be very similar. From earlier FT IR studies, it is known that, below the main phase transition, the trans population at the deuterated position C-6 is higher than 95%.<sup>8</sup> As a consequence, trans–gauche isomerization does not play an important role for the experimental  $^2\text{H}$  NMR line shape effects and  $T_2$  relaxation of the DPPG<sub>2</sub> samples below the main transition. Using the model of anisotropic rotational diffusion in an ordering potential,<sup>32,34–37</sup> we were able to reproduce both the experimental  $^2\text{H}$  NMR line shapes and the  $T_2$  relaxation data. In general, the derived rate constants for the rotation of the lipid molecules around their long molecular axes are found to be of the same order as those discussed for DMPC bilayers.<sup>34–36</sup>

Pure DPPG<sub>2</sub>/water bilayers and the mixture with cholesterol, however, show almost identical rate constants, whereas for DMPC, the lipid overall rotation is slowed by about 1 order of magnitude upon addition of 40 mol % cholesterol.<sup>6,35</sup> Moreover, the activation energy of 46.1 kJ/mol for overall rotation in pure DPPG<sub>2</sub> bilayers is lower than in pure DMPC bilayers, where values between 60 and 90 kJ/mol are discussed.<sup>6,34–36,47</sup> These results can be related to the bulkier diglycerol headgroup and to its anionic character that increases the lipid–lipid distance and thus facilitates long axis rotation. Addition of 40 mol % cholesterol increases the membrane fluidity, as expressed by a smaller activation energy for chain rotation (28.8 kJ/mol). This is in agreement with the findings for DMPC/cholesterol mixtures for which the same activation energy was reported.<sup>6</sup>

The rate constants for molecular fluctuations of the phospholipids are found to be nearly the same for both DPPG<sub>2</sub> samples and are almost 2 orders of magnitude smaller than those in DMPC bilayers.<sup>6,35,47</sup> The high activation energies of 82.9 and 80.5 kJ/mol for the pure bilayers and DPPG<sub>2</sub>/cholesterol mixture, respectively, are very close to those of the corresponding DMPC bilayers (pure DMPC bilayers, 90 kJ/mol; DMPC/cholesterol mixtures, 80 kJ/mol).<sup>6,35</sup> These observations are attributed to the hydrophilicity of the diglycerol headgroup, which, because of hydration, becomes rather bulky and thus reduces the influence of cholesterol on the chain fluctuations. In addition, the lipid fluctuation in DPPG<sub>2</sub> is strongly hindered, which can be deduced from the considerably smaller rate

constants in these systems as compared to the corresponding DMPC systems.

At this point, it is worthwhile to comment on the results from the  $^{31}\text{P}$   $T_2$  relaxation experiments. The slope on both sides of the low-temperature minimum of the  $^{31}\text{P}$   $T_2$  relaxation curve indicates a surprisingly high activation energy of about 150 kJ/mol. This observation can be understood by the fact that, at about 273 K, the surrounding water freezes out and hence affects the dynamics of the headgroup region, which is dominated by the rotational motion around the molecular long axis.<sup>47</sup> The large difference between the activation energy for the rotational motion of the acyl chains (46.1 kJ/mol,  $^2\text{H}$  NMR data, see above) and for the headgroup region ( $^{31}\text{P}$   $T_2$  data) implies that the hydrophobic part, i.e., the acyl chain region, is at least partially decoupled from the phosphate headgroup, with the latter being directly influenced by the actual state of the surrounding water molecules.

The common low-temperature  $^2\text{H}$   $T_1$  minimum of the present DPPG<sub>2</sub> samples cannot be attributed to the aforementioned reorientational chain motions. Rather, it indicates a unique feature of the C-2 segment in the *sn*-2-chain that—as discussed during previous studies—is given by jumps between gauche<sup>+</sup> and gauche<sup>−</sup> conformational states at carbon position C-2, i.e., rotation around the C-2–C-3 bond of the acyl chain.<sup>35,42</sup> The rate constants and activation energies for this internal motional contribution in DPPG<sub>2</sub> bilayers are in line with earlier reports.<sup>35</sup> Above 295 K, the situation, however, is further complicated by the fact that trans–gauche isomerization at carbon position C-6 as well as overall chain reorientation enter the time scale for  $T_1$  relaxation. An unequivocal analysis of the  $^2\text{H}$   $T_1$  relaxation data was therefore not possible in this temperature range.

In conclusion, it can be stated that, unlike the situation in DMPC bilayers, in DPPG<sub>2</sub>/water dispersions, the presence of cholesterol is of minor importance for the actual lipid mobility. Rather, it seems that the diglycerol headgroup has a dominant influence on the lipid dynamics, as it gives rise to a lower packing density in the acyl chain region. The hydrated, bulky headgroup also is responsible for the observed decoupling between the headgroup and acyl chain dynamics.

**Chain Order.** The derived order parameter  $S_{\text{CD}}$  of the present DPPG<sub>2</sub> bilayers is significantly lower than the values derived for related systems. For instance, in pure DPPC bilayers, values between 0.2 (323 K) and 0.16 (353 K) are reported.<sup>15</sup> This reduction of the chain order in DPPG<sub>2</sub> is attributed to the anionic character and to the high hydrophilicity of the diglycerol headgroup, whose overall size increases considerably upon hydration. As a result, the packing density in the acyl chain region is reduced, as reflected by the lower chain order parameter  $S_{\text{CD}}$ .

In quite the same way, the orientational order parameter  $S_{\alpha}$  of pure DPPG<sub>2</sub>/water bilayers is found to be significantly lower than the values obtained for DMPC<sup>6,35,47</sup> or DPPC bilayers,<sup>8</sup> where  $S_{\alpha}$  values between 0.6 and 0.75 are reported in the liquid crystalline phase. In the gel phase, the differences between the various lipid systems are less pronounced. Nevertheless, the limiting value of 0.9 in DPPG<sub>2</sub> is lower than for DMPC with a limiting value for  $S_{\alpha}$  of 1.0.<sup>6</sup> The incorporation of 40 mol % cholesterol has a significant influence on the orientational order. At low temperatures—because of the distortion of the lipid chain packing—the addition of cholesterol leads to a slight decrease of the order parameter  $S_{\alpha}$ , which prevents the membrane from forming the gel phase. At the main phase transition temperature of the pure lipid bilayers, only a slight discontinuity is observed. Thus, at  $T > 314$  K, the orientational order parameter  $S_{\alpha}$  is



found to be higher than that for the pure lipid/water dispersion. The values, however, are significantly lower than reported for DMPC<sup>6,35,47</sup> or DPPC bilayers,<sup>8</sup> which exhibit values of about 0.75–0.9. Again, this low orientational order in DPPG<sub>2</sub>/cholesterol can be traced back to the larger hydration of the diglycerol headgroup, which prevents a close molecular packing and gives rise to a greater conformational and motional freedom of the lipid molecules. The rigid cholesterol increases the conformational order and minimizes the lipid fluctuation amplitude, as reflected by the enhanced conformational and orientational order parameters. Nevertheless, because of the larger headgroup of DPPG<sub>2</sub>, the addition of cholesterol is not sufficient to achieve a similar high packing density as in DMPC or DPPC bilayers upon addition of cholesterol.

The derived segmental order parameter  $S_\gamma$  for the complete acyl chain (see Figure 7) shows a pronounced temperature dependence and a characteristic gradient along the chain, starting from a more ordered plateau region in the vicinity of the glycerol backbone toward the less ordered chain end (position C-16). Again, the ordering effect of cholesterol is expressed by an increasing segmental order parameter  $S_\gamma$ . However, it should be noted that the order parameter  $S_\gamma$  cannot be used to calculate directly the exact gauche probability at a particular CD<sub>2</sub> segment as implied by eqs 4 and 5, which are based on the assumption that only kink conformers exist. That is, the <sup>2</sup>H NMR data do not account for double-gauche or single-gauche conformers, which cause an inclination of the chain relative to the long molecular axis. This inclination changes the C–D bond angles for all subsequent CD<sub>2</sub> segments and results in a seemingly higher gauche population. This effect is more pronounced toward the acyl chain end, where the probability of single- and double-gauche conformers is higher.

The generally lower conformational order in DPPG<sub>2</sub> bilayers is also reflected by the results for the effective chain lengths. Here, for pure DPPG<sub>2</sub>/water bilayers, values of about 11.5 Å are observed, which are considerably lower than those of DPPC/water bilayers, where values of about 13.5 Å are reported.<sup>15,46</sup> The comparison of the various theoretical approaches reveals that the methods of Seelig et al.<sup>13,14,45</sup> and Chan and Oldfield<sup>12,44</sup> are very similar, where the latter one—which also accounts for overall lipid fluctuations—provides somewhat shorter chain lengths. The first-order mean-torque model<sup>15,46</sup> provides the lowest values over the whole temperature range. The largest deviation between the data from the mean-torque model and the other approaches are registered at higher sample temperatures, which is a consequence of the low order parameters  $S_{CD}$ .

The incorporation of 40 mol % cholesterol leads to an increase of the effective chain length by about 15%, which is a direct consequence of the higher conformational order in the liquid ordered phase. It is quite obvious that, for DPPG<sub>2</sub>/cholesterol mixtures, the deviations between the data from the first-order mean-torque model<sup>15,46</sup> and those from the other two approaches are much smaller, which—as shown by model calculations—is directly related to the generally higher  $S_{CD}$  values. Obviously, at higher chain orders, similar effective chain lengths are derived that are almost independent of the actual underlying theoretical approach.

## Conclusions

In the present work, lipid bilayers containing a new synthetic phospholipid, DPPG<sub>2</sub>, were investigated for the first time by variable-temperature <sup>2</sup>H and <sup>31</sup>P NMR spectroscopy to determine the ordering characteristics and dynamic properties of the lipid molecules as a function of temperature and sample composition.

A thorough analysis of the <sup>2</sup>H NMR data provided the kinetic parameters of the overall lipid reorientation (modeled by anisotropic rotational diffusion), and gauche<sup>+</sup>–gauche<sup>−</sup> isomerization at carbon C-2 in the gel phase as well as of the lateral diffusion in the liquid crystalline phase. It could be demonstrated that the bulky diglycerol headgroup plays a dominant role for the actual motional characteristics of the lipid molecules in the present bilayers. Obviously, the lower packing density in DPPG<sub>2</sub> bilayers results in a less hindered overall mobility (viz., rotational and lateral motions) of the lipid molecules as compared with typical phospholipids, such as DMPC or DPPC.

Starting from the order parameter  $S_{CD}$ , determined via <sup>2</sup>H NMR experiments on samples with selectively deuterated acyl chains, we were able to determine the orientational order parameter  $S_\alpha$  as well as the segmental order parameter  $S_\gamma$ .  $S_\alpha$  could be determined via computer simulations of the <sup>2</sup>H NMR data in the gel phase and via combined FT IR/<sup>2</sup>H NMR data in the liquid crystalline region. With these  $S_\alpha$  values and the  $S_{CD}$  data from measurements on samples containing perdeuterated acyl chains, it was possible to calculate the segmental order parameter  $S_\gamma$  for every position along the acyl chains. In addition, on the basis of these known order parameters, the effective acyl chain length as a projection onto the director could be determined as a function of both temperature and cholesterol content.

On the basis of these data, it is concluded that the orientational as well as segmental order in these DPPG<sub>2</sub> bilayers are significantly lower as compared to those in DPPC or DMPC, which can be traced back to the higher hydration of the negatively charged headgroup. As a further consequence, the reduced conformational order directly yields a significant shortening of the effective acyl chain length.

The question arises as to whether the observed differences in lipid mobility and lipid order of the present DPPG<sub>2</sub> membranes are in fact related to the unusual stability, i.e., longer blood circulation times, of the corresponding liposomes, which, in addition to DPPC and cholesterol, contain DPPG<sub>2</sub> as a major structural component. Preliminary results from recent NMR studies on “real” mixtures, however, have indicated a very similar behavior for the DPPG<sub>2</sub> component as found in the present work. The present NMR studies on DPPG<sub>2</sub> and DPPG<sub>2</sub>/cholesterol bilayers thus are a prerequisite for the forthcoming analysis of the aforementioned more complex bilayer mixtures. The corresponding spectroscopic studies on these mixtures are in progress.

**Acknowledgment.** Financial support for this project by the Deutsche Forschungsgemeinschaft and the Fonds der Chemischen Industrie (FCI) is gratefully acknowledged. The authors thank Mrs. D. Zausser and Mrs. G. Bräuning for their help during the synthesis of the deuterated compounds.

## Appendix: Calculation of the Effective Acyl Chain Lengths

On the basis of the derived order parameters, the effective chain length (in angstroms) was derived using three different theoretical approaches: (i) the model of Petersen and Chan<sup>12</sup> and Oldfield,<sup>44</sup> (ii) the diamond-lattice model of Seelig et al.,<sup>13,14,45</sup> and (iii) the first-order mean-torque model of Petrache et al.<sup>15,46</sup>

In the first approach,<sup>12,44</sup> it is assumed that  $S_\gamma$  reflects the probability that a bond is in a gauche isomeric state, using eqs 4 and 5. Moreover, a rigid body fluctuation with an order parameter  $S_\alpha$ , describing the most probable fluctuation amplitude

$\alpha_0$ , is considered. Here, for the order parameter  $S_\alpha$ , the following distribution function holds<sup>12</sup>

$$S_\alpha = \frac{1}{2} \frac{\int_0^\pi (3\cos^2\alpha - 1) \exp\left[-\frac{1}{2}\left(\frac{\alpha}{\alpha_0}\right)^2\right] \sin\alpha \, d\alpha}{\int_0^\pi \exp\left[-\frac{1}{2}\left(\frac{\alpha}{\alpha_0}\right)^2\right] \sin\alpha \, d\alpha} \quad (7)$$

We then follow the procedure from Oldfield et al.<sup>44</sup> to calculate the projection of a single C–C segment  $\langle l_i \rangle$  and of the whole acyl the chain (= effective chain length)  $\langle L \rangle$  onto the director

$$\begin{aligned} \langle l_i \rangle &= 1.25[p_t + p_g \cos(60^\circ)] \cos \langle \alpha \rangle \\ \langle L \rangle &= \sum_{i=2}^{n_c-1} \langle l_i \rangle \end{aligned} \quad (8)$$

$p_t$  and  $p_g$  are the gauche and trans probabilities of the  $i$ th segment, as derived from the corresponding order parameter  $S_\gamma$ , and  $n_c$  is the number of acyl chain segments (here,  $n_c = 16$ ).

The second model was proposed by Seelig et al.<sup>13,14,45</sup> In this case, the overall order parameter  $S_{CD}$  is completely traced back to internal conformational isomerization, whereas rigid body motions are neglected. It is assumed that the C–D bond orientations fall on a tetrahedron lattice with  $0^\circ$ ,  $60^\circ$ , and  $90^\circ$ , whereas the angles  $120^\circ$  and  $180^\circ$  are not taken into account because of the back-folding of the chains. The order parameter  $S_{CD}$  therefore is given by

$$S_{CD} = p_0 S_{90} + \frac{1}{2} p_{60} (S_{35.3} + S_{90}) + p_{90} S_{35.3} \quad (9)$$

Here,  $p_\alpha$  is the probability that a segment is oriented at the angle  $\alpha$ . From this expression, the effective chain length is readily calculated as

$$\langle L \rangle = 1.25 \left[ \frac{n_c - 1}{2} + \sum_{i=2}^{n_c-1} |S_{CD}^i| \right] \quad (10)$$

As a third, independent approach, the mean-torque model<sup>15,46</sup> was used, which is based on a continuum model of segmental orientations. In a first approximation, slower, overall motions are neglected. The conformational order for each chain segment is then expressed by a mean-field orientational potential, which is expanded into a Legendre polynomial. Here, a distribution function is written as follows

$$f(x) = \frac{\exp(\epsilon_1 x + \epsilon_2 x^2)}{\int_{-1}^1 \exp(\epsilon_1 x + \epsilon_2 x^2) \, dx} \quad (11)$$

The parameters  $\epsilon_1$  and  $\epsilon_2$  cannot be calculated independently. Normally, the parameter  $\epsilon_2$  is neglected, and  $\epsilon_1$  is assumed to be the dominant term (“first-order mean-torque model”) for large  $S_{CD}$  values. The average projection  $\langle x \rangle$  of a particular methylene segment is obtained by solving the following equations for a given  $\langle x^2 \rangle$

$$\langle x \rangle = \coth(\epsilon_1) - \frac{1}{\epsilon_1}, \quad \langle x^2 \rangle = 1 + \frac{2}{\epsilon_1^2} - \frac{2}{\epsilon_1} \coth(\epsilon_1) \quad (13)$$

The quantity  $\langle x^2 \rangle$  is connected to the order parameter  $S_{CD}$ . Further details are described in refs 15 and 46.

## References and Notes

- (1) Seelig, J.; Seelig, A. *Q. Rev. Biophys.* **1980**, *13*, 19.
- (2) Griffin, R. G. *Methods Enzymol.* **1981**, *72*, 108.
- (3) Davis, J. H. *Biochim. Biophys. Acta* **1983**, *737*, 117.
- (4) Davis, J. H. *Adv. Magn. Res.* **1989**, *13*, 195.
- (5) Evans, J. N. *Biomolecular NMR Spectroscopy*; Oxford University Press: Oxford, U.K., 1995.
- (6) Weisz, K.; Gröbner, G.; Mayer, C.; Stohrer, J.; Kothe, G. *Biochemistry* **1992**, *31*, 1100.
- (7) Davies, M. A.; Hübner, W.; Blume, A.; Mendelsohn, R. *Biochemistry* **1990**, *29*, 4368.
- (8) Lehnert, R.; Eibl, H.-J.; Müller, K. *J. Phys. Chem. B* **2003**, *107*, 75.
- (9) Wolfangel, P.; Müller, K. *J. Phys. Chem. B* **2003**, *107*, 9918.
- (10) Maroncelli, M.; Strauss, H. L.; Snyder, R. G. *J. Chem. Phys.* **1985**, *82*, 2811.
- (11) Mendelsohn, R.; Davies, M. A.; Schuster, H. F.; Dluhy, R. A. *Biochemistry* **1989**, *28*, 8934.
- (12) Petersen, N. O.; Chan, S. I. *Biochemistry* **1977**, *16*, 2657.
- (13) Seelig, A.; Seelig, J. *Biochemistry* **1974**, *13*, 4839.
- (14) Schindler, H.; Seelig, J. *Biochemistry* **1975**, *14*, 2283.
- (15) Petrache, H. I.; Tu, K.; Nagle, J. F. *Biophys. J.* **1999**, *76*, 2479.
- (16) Allen, M. T.; Chonn, A. *FEBS Lett.* **1987**, *223*, 42.
- (17) Klibanow, A.; Muruyama, K.; Torchilin, V. P.; Huang, L. *FEBS Lett.* **1990**, *268*, 235.
- (18) Klibanow, A.; Muruyama, K.; Beckerleg, A. M.; Torchilin, V. P.; Huang, L. *Biochim. Biophys. Acta* **1991**, *1062*, 142.
- (19) Allen, T. M.; Hansen, C.; Martin, F.; Redemann, C.; Yau-Yong, A. *Biochim. Biophys. Acta* **1991**, *1066*, 29.
- (20) Allen, T. M.; Hansen, C. *Biochim. Biophys. Acta* **1991**, *1068*, 133.
- (21) Allen, T. M. In *Liposomes: The Therapy of Infectious Diseases and Cancer*; Lopez-Berestein, G., Fidler, I., Eds.; Alan R. Liss Inc.: New York, 1989; p 405.
- (22) *Organikum*, 16. Auflage; VEB Verlag der deutschen Wissenschaften: Berlin, 1986.
- (23) Norman, R. O. C.; Coxon, J. M. *Principles of Organic Synthesis*; Blackie Academic and Professional: London, 1993.
- (24) Zimmermann, H. *Liq. Cryst.* **1989**, *4*, 591.
- (25) Woolley, P.; Eibl, H. *Chem. Phys. Lipids* **1988**, *47*, 55.
- (26) Eibl, H. *Chem. Phys. Lipids*, manuscript in preparation.
- (27) Maruyama, K.; Okuizumi, S.; Ishida, O.; Yamuchi, H.; Kikuchi, H.; Iwatsumi, M. *Int. J. Pharm.* **1994**, *111*, 103.
- (28) Eibl, H.; Schargon, O.; Erdleubrich, B. *Chem. Phys. Lipids*, manuscript in preparation.
- (29) Heaton, N. J.; Vold, R. R.; Vold, R. L. *J. Magn. Reson.* **1988**, *77*, 572.
- (30) Schmider, J.; Müller, K. *J. Phys. Chem. A* **1998**, *102*, 1181.
- (31) Liebelt, A.; Detken, A.; Müller, K. *J. Phys. Chem. B* **2002**, *106*, 7781.
- (32) Villanueva-Garibay, A.; Müller, K. *Lecture Notes in Physics*, 2004, in press.
- (33) Moro, G.; Segre, U.; Nordio, P. L. In *Nuclear Magnetic Resonance of Liquid Crystals*; D. Reidel: Dordrecht, The Netherlands, 1990.
- (34) Meier, P.; Ohmes, E.; Kothe, G.; Blume, A.; Weidner, J.; Eibl, H. *J. Phys. Chem.* **1983**, *87*, 4904.
- (35) Mayer, C.; Müller, K.; Weisz, K.; Kothe, G. *Liq. Cryst.* **1988**, *3*, 797.
- (36) Meier, P.; Ohmes, E.; Kothe, G. *J. Phys. Chem.* **1986**, *85*, 3598.
- (37) Müller, K.; Meier, P.; Kothe, G. *Prog. NMR Spectrosc.* **1985**, *17*, 211.
- (38) Saupe, A. *Z. Naturforsch.* **1964**, *19A*, 161.
- (39) Fenske, D. B.; Jarrell, H. C. *Biophys. J.* **1991**, *59*, 55.
- (40) Wefing, S.; Kaufmann, S.; Spiess, H. W. *J. Chem. Phys.* **1988**, *89*, 1234.
- (41) Wolfangel, P.; Meyer, H. H.; Bornscheuer, U. T.; Müller, K. *Biochim. Biophys. Acta* **1999**, *1420*, 121.
- (42) Fuson, M. M.; Prestegard, J. H. *Biochemistry* **1983**, *22*, 1311.
- (43) Ipsen, J. H.; Mouritsen, O. G.; Zuckermann, M. *Biophys. J.* **1989**, *56*, 661.
- (44) Oldfield, E.; Meadows, M.; Rice, D.; Jacobs, R. *Biochemistry* **1978**, *17*, 2727.
- (45) Seelig, J.; Seelig, A. *Q. Rev. Biophys.* **1980**, *13*, 337.
- (46) Petrache, H. I.; Dodd, S. W.; Brown, M. F. *Biophys. J.* **2000**, *79*, 3172.
- (47) Dufourc, E.; Mayer, C.; Stohrer, J.; Althoff, G.; Kothe, G. *Biophys. J.* **1992**, *61*, 42.
- (48) Cevc, G., Ed. *Phospholipids Handbook*; Marcel Dekker: New York, 1993.
- (49) Lindblom, G.; Orädd, G. *Prog. NMR Spectrosc.* **1994**, *26*, 483.
- (50) Crawford, M. S.; Gerstein, B. C.; Kuo, A.; Wade, C. G. *J. Am. Chem. Soc.* **1980**, *102*, 3728.
- (51) Vaz, W. L. C.; Clegg, R. M.; Halmann, D. *Biochemistry* **1985**, *24*, 781.
- (52) Vaz, W. L. C.; Halmann, D.; Clegg, R. M.; Gambacorta, A.; DeRosa, M. *Eur. Biophys. J.* **1975**, *12*, 19.